The magnetic phase diagram of $Mn_xZn_{1-x}PS_3$

1998 J. Phys.: Condens. Matter 10 7643

(http://iopscience.iop.org/0953-8984/10/34/017)

J. Phys.: Condens. Matter **10** (1998) 7643–7652. Printed in the UK PII: S0953-8984(98)92934-4

The magnetic phase diagram of $Mn_xZn_{1-x}PS_3$

D J Goossens† and T J Hicks

Physics Department, Monash University, Clayton, 3168, Victoria, Australia

Received 1 April 1998, in final form 10 June 1998

Abstract. The magnetic phase diagram for $MnPS_3$ is established, and then explored with regard to Zn substitution at the Mn sites. This allows construction of the temperature/applied-field/dilution phase diagram. Furthermore, it is concluded that second- and third-nearest-neighbour interactions are important in determining the magnetic behaviour of the system.

1. Introduction

The behaviour of two-dimensional (2D) magnetic systems has received a great deal of attention [1]. Theoretically, problems that are difficult in three dimensions often become more tractable in two dimensions. The classic example is the Onsager solution to the 2D rectangular Ising model [2]. Thus, the study of low-dimensional magnets allows these models to be experimentally realized, and gives new insights into fundamental phenomena. In the study of 2D antiferromagnets, systems such as X_2YF_4 where X may be Rb or K and Y maybe be Mn, Co, Ni for example [1, 3, 4] are most commonly studied. In addition, the parent materials of copper–oxygen-based superconductors are often 2D antiferromagnets [5]. In all of these cases the 2D lattice is square. Manganese thiophosphate, $MnPS_3$, is a honeycomb-lattice material, and therefore opens up new and unusual possibilities for study.

In this paper, we construct and explore the temperature/applied-field/magnetic dilution phase of $MnPS_3$. It is a layered, quasi-two-dimensional Heisenberg antiferromagnet with, at low applied fields, a small anisotropy causing the moments to point in the z-direction—perpendicular to the layer planes. The Néel temperature, T_N, is 78 K at low fields ($H_z < 40$ kOe, where H_z is applied in the z-direction) [6]. Crystallographically, it is a monoclinic structure with space group $C2/m$ and lattice parameters $a = 6.077$ Å, $b = 10.524$ Å, $c = 6.796$ Å and $\beta = 107.35^\circ$, so the c-axis is not quite parallel to the z-direction. In the layers, manganese atoms form a honeycomb lattice, with each manganese neighboured by three manganese atoms and three P_2 pairs [7]. Each layer is sandwiched within a pair of sulphur layers. These three-layer structures are then held together by Van der Waals forces between adjacent sulphur layers. The distance between manganese layers and the associated complex exchange path are the factors that give rise to the two-dimensional magnetism exhibited by $MnPS_3$ and other transition metal thiophosphates.

Each manganese atom is antiferromagnetically linked ($J_1/k \sim$ 8–10 K) [8, 9] to its three intraplanar nearest neighbours, and ferromagnetically linked to its interplanar nearest neighbours [6] (figure 1). The best current estimate of the ratio of interplanar (J') to

† Author to whom any correspondence should be addressed; telephone: +61 3 9905 3620; fax: +61 3 9905 3637; e-mail: darren.goossens@sci.monash.edu.au.

0953-8984/98/347643+10$19.50

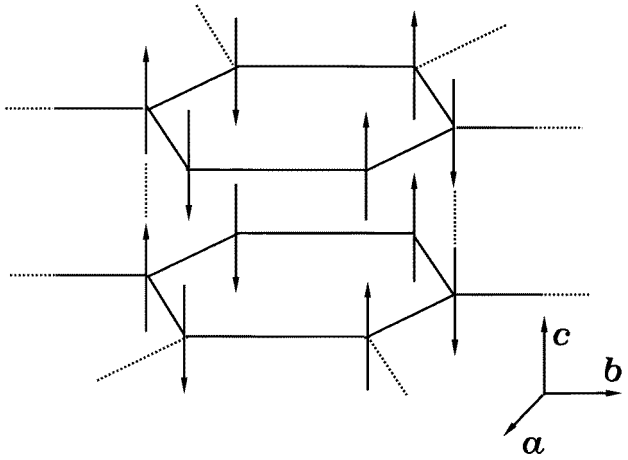

Figure 1. The spin structure of $MnPS_3$. Arrows denote spin directions.

intraplanar first-neighbour exchange (J_1) is of the order of 1/400 [10]. Previous results include an estimate of 2/5 [9], but these measurements are more doubtful. So $MnPS_3$ is a useful approximation to a 2D magnet.

In this paper, we will present the phase diagram of $MnPS_3$ as a function of temperature, field and dilution of the magnetic atoms by means of substitution of a non-magnetic species, in this case zinc. Zinc was chosen because $ZnPS_3$ is of the same structure, with lattice parameters that are very similar to those of $MnPS_3$ [7]. $Mn_xZn_{1-x}PS_3$ is explored in [8], which establishes that the Curie–Weiss temperature is a linear function of x, suggesting that Zn does substitute randomly in the system. It also establishes that the system's susceptibility can be effectively explained using high-temperature series expansions for x greater than the percolation value, and fitted by adding in a Curie correction when x is below the percolation value. This correction scales with x. Thus, the susceptibility arising from antiferromagnetic order is still significant for x less than the critical concentration.

2. Sample preparation and apparatus

Samples of $Mn_xZn_{1-x}PS_3$ were prepared for $x = 1$, 0.95, 0.8, 0.65, 0.5 and 0.3 using a vapour-transport method. Stoichiometric quantities of 99.99% pure elements were sealed in a quartz tube under $\sim 10^{-6}$ Torr of argon. The 18 cm tube was then placed in a two-zone furnace, with the temperature varying smoothly from 700 to 680 °C along the length of the tube. This produced a mass of transparent green crystals of hexagonal habit, typical dimensions being $5 \times 5 \times 0.1$ mm. X-ray diffraction and microprobe analysis confirmed the structure and composition.

Measurements were taken using a Quantum Design MPMS-7 SQUID magnetometer, capable of applying fields from -70 to $+70$ kOe and temperatures of 2 to 350 K. Samples were mounted with the planes either horizontal, if the parallel susceptibility, $\chi_{\parallel}$, was to be measured (with the c-axis approximately parallel to applied field, $H = H_z$), or with the planes vertically oriented, for measurements of $\chi_{\perp}$ (with the c-axis approximately perpendicular to $H = H_{xy}$).

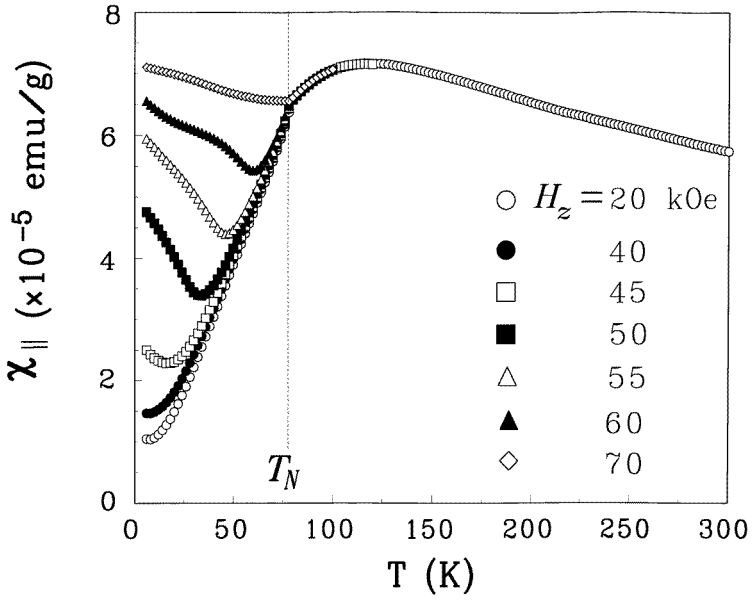

Figure 2. The parallel susceptibility of $MnPS_3$ as a function of temperature at different applied fields, H_z.

3. $MnPS_3$

Initial investigations confirmed that $T_N = 78$ K for $MnPS_3$ when the applied field, H, was either parallel to the moment direction (perpendicular to the layers) or perpendicular to the moment direction. Initial measurements were taken in fields of 100, 600 and 10 000 Oe, and demonstrated little variation across fields, and showed only minor differences between field-cooled and zero-field-cooled runs. Maximum susceptibilities were typically 7×10^{-5} emu g^{-1}, and any variations in magnitudes could be accounted for by uncertainties in the sample masses. Figure 2 shows χ versus T at different fields applied along the spin direction ($H = H_z$). T_N is determined from the discontinuity in the first derivative $(\partial M/\partial T)_H$. The hump at 120 K ($T \sim (3/2)T_N$) is characteristic of the persistence of short-range order within the planes of a 2D magnet [1]. Fitting the high-temperature series expansion of Rushbrooke and Wood [11] to these data gave a nearest-neighbour exchange of $J_1/k = 8.1$ K, with excellent reliability and in excellent agreement with recent results [8].

The negative gradient of $\chi_{\perp}$ as T increases from zero can be attributed to spin waves [12].

These measurements show that the susceptibility behaves like the parallel susceptibility ($\chi_{\parallel}$) of an ordered antiferromagnet at small H_z, with its positive temperature dependence, to a $\chi_{\perp}$-behaviour at high fields where the susceptibility shows a much weaker and slightly negative temperature dependence. This indicates a spin flop taking place at $H_z \sim 45$ kOe at low temperatures. This is graphically illustrated in the runs carried out between 45 and 60 kOe, where the susceptibility shows a $\chi_{\perp}$-shape at low temperatures and becomes more $\chi_{\parallel}$-like as T_N is approached. The point on the χ versus T curve where the gradient takes on its most negative value gives the temperature of the spin flop at that field, as this is where the moments are changing orientation most rapidly. Thus, H_{sf} increases as T increases, a result which will be shown in greater detail when spin-flop curves are discussed.

Figure 2 also shows that T_N maintains considerable consistency across fields. This is not unexpected, as measurements must be taken very close to the critical point if critical behaviour is to be seen. T_N did not vary appreciably, even in experiments with the applied field very close to the value taken on by H_{sf} in the vicinity of T_N. Theories of the magnetic phase diagram [13, 14] suggest that T_N should decrease markedly near $H_z = H_{sf}$, as at H_{sf} the anisotropy, which gives rise to the ordering, is suppressed by the external field. However, in an imperfect 2D magnet, ordering can also arise through the interplanar coupling or distant-neighbour interactions. Thus, despite the lower dimensionality, no large reduction in T_N is seen. In [15], a second magnetic order, with spins lying parallel to the *b*-axis, was observed above T_N. This suggests a small in-plane anisotropy, which could also be responsible for maintaining order.

When a magnetic field H_z is applied parallel to the easy axis—parallel with the anisotropy direction—there will be two competing interactions—the anisotropy, denoted DS^2, and the Zeeman energy $\frac{1}{2}(\chi_\perp - \chi_{||})H_z^2$ [13]. For small H_z, the moments will remain in the z-direction. But as the Zeeman energy increases with field, the two terms will come to be equal. The field at which this happens is the spin-flop field, H_{sf}. Therefore H_{sf} can give the anisotropy. This anisotropy is the result of competing single-ion and dipolar anisotropies, with the dipolar effects being the stronger [9, 17].

At the spin-flop field, the moments flop from the antiparallel Ising-like antiferromagnetic (AF) arrangement in which they are perpendicular to the planes, to an antiparallel spin-flop (SF) arrangement within the planes, as the magnet is now an easy-plane magnet due to an effective change in the sign of the anisotropy. The spins, however, are still Heisenberg spins. A Kosterlitz–Thouless bound vortex phase [16] is unlikely in $MnPS_3$. This is because of interplanar and possible next-nearest-neighbour interactions, and the possibility of a preferred direction within the planes [10, 15], all of which may allow the flopped phase to order in a truly long-range fashion. This agrees with the observed $\chi_{||}$ versus T data at

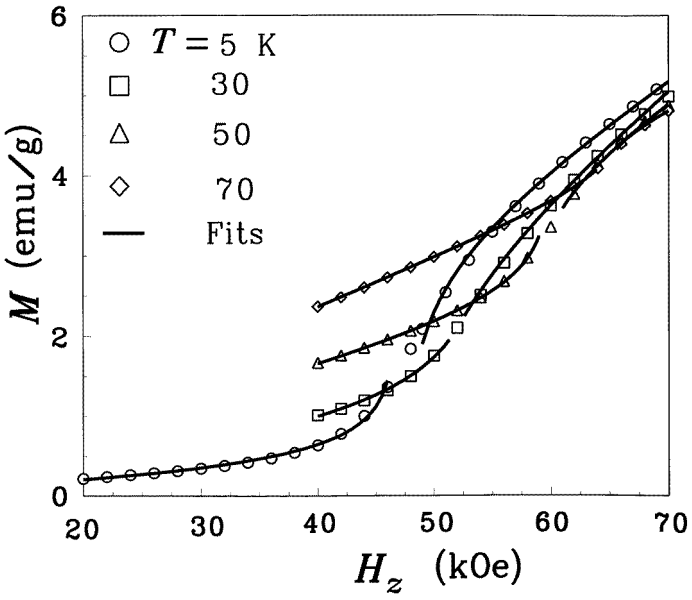

Figure 3. Spin-flop curves for $MnPS_3$ at various temperatures. The fits to the soliton theory are shown as solid lines.

high fields in which $\chi_\parallel$ behaves like a true transverse susceptibility.

Measurements were made of magnetic moment versus H_z at constant temperature for temperatures varying from 5 K to T_N. A typical series of such runs can be seen in figure 3. The response can be seen to be linear with field, and then to increase rapidly before again reaching a linear regime. What is happening is that initially the spins are parallel to the applied field. The 5 K curve in figure 2 shows $\chi_\parallel$ at this temperature to be very small—hence the small gradient of the M versus H_z curve for $H_z < H_{sf}$. But as H_z increases, as noted above, the spins flop into the plane. As they are now perpendicular to the applied field, they show a $\chi_\perp$-response, which figure 2 shows is much stronger—hence the larger gradient of the M versus H_z curve for $H_z > H_{sf}$. As noted above, the spin-flop field increases with temperature, as expected given that $\chi_\perp - \chi_\parallel$ is decreasing.

The spin flops in figure 3 show considerable width—10 kOe—greater by an order of magnitude than widths due to demagnetizing effects or the applied field being at a small angle to the z-direction [13]. This is evidence of the two dimensionality smearing out the transition. Because of the high order of the transitions, H_{sf} is found by taking the maximum in the derivative $(\partial M/\partial H)_T$.

Fitting the H_{sf} versus T data thus obtained allowed an extrapolation to be made to find $H_{sf}(T = 0)$, which was found to be 45 kOe. This is different from the values obtained in [9] of 36.6 kOe and in [18] of 38 kOe. This value is larger by approximately 20%. However, the value showed consistency across samples from different crystal growth runs, and the analysis of the samples could find nothing amiss. Furthermore, this H_{sf} fits well into the H_{sf} versus magnetic dilution data discussed in section 4. The reason for the discrepancy is unclear.

The spin-flop curves can be fitted by a soliton theory [1, 13]. In this theory, the spin-flop phase is nucleated by domain walls, as within a wall the spins change orientation, and so there will be spins lying in the planes even at low fields. As H_z is increased, the domain wall width diverges—the ratio of flopped to unflopped phase increases. Therefore, this theory can lead to a prediction for the magnetization as a function of field at a given temperature. Reference [13] gives

$$M_{sol} = 8S^2\chi_\perp H_z \left[\frac{2|J_1|^{3/2}}{\pi k_B T|D(1 - H_z^2/H_{sf}^2)|^{1/2}}\right]^{1/2} q^{-1} \tag{1}$$

which leads to the magnetization being given by

$$\begin{aligned} M &= M_{sol} && (H_z < H_{sf}) \\ M &= \chi_\perp H_z - M_{sol} && (H_z > H_{sf}) \end{aligned} \tag{2}$$

where M_{sol} is the contribution of the spins in a static domain wall to the magnetization. q^{-1} is a domain wall density, J_1 is the nearest-neighbour exchange and S is the spin. As we can find D from H_{sf} and the susceptibilities can be measured, q^{-1} is the only unknown. This allows a useful test of the theory. The solid lines in figure 3 show the results of fitting (2) to various spin flops. In the fit, q and a background term linear in H_z are the only variable parameters. The soliton fit assumes that M is due solely to spins in the domain walls. The linear term allows for the response of spins in the domains themselves. This is necessary, as unpaired spins are possible in a honeycomb lattice due to the odd number of nearest neighbours. All of the other values are taken from previous experiments, and as can be seen the resulting fit is quite acceptable, an encouraging sign of consistency.

The fit gives $q^{-1} \sim 0.003$, at 5 K—a reasonable figure [13], given that q measures the distance in lattice spacings between domain walls and that typical values are 10^{-3} for K_2MnF_4 [1]. Note that the fit is useful until quite close to the spin flop itself. The coefficient

of the linear term changed from 9×10^{-6} emu g^{-1} for $H_z < H_{sf}$ to 4×10^{-5} emu g^{-1} for $H_z > H_{sf}$, indicating that not all of the magnetization is due to the domain walls. Unpaired spins within domains are the likely cause, as this agrees with the larger susceptibility for the perpendicular arrangement.

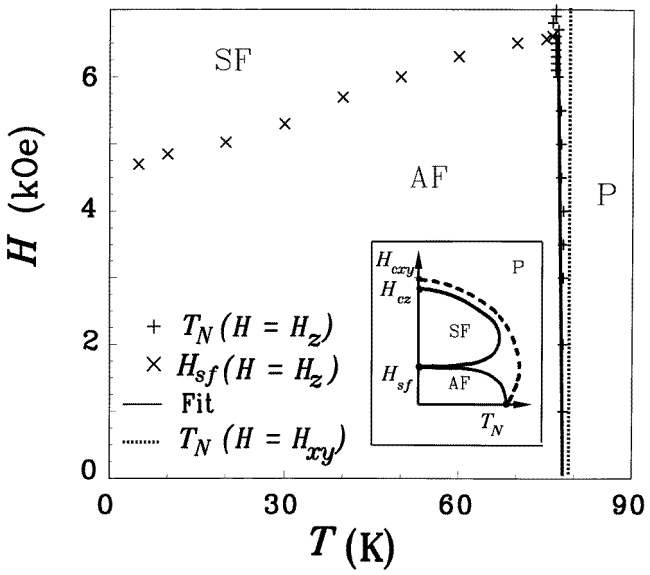

Figure 4. The magnetic phase diagram of $MnPS_3$. SF, AF and P denote spin-flop, antiferromagnetic and paramagnetic phases respectively.

Figure 4 shows the phase diagram derived for pure $MnPS_3$. This agrees in general with the theoretical diagram (figure 4, inset) [13]. However, in the experimental case, T_N remains more constant with field. It appears to decrease by just one degree in the vicinity of H_{sf}, rather than retreating to zero. The true extent may well be masked by SQUID resolution, because if the spin-flop line is truly bifurcating, the gap between the two lines after bifurcation may be unmeasurable until temperatures well in excess of the temperature of the bicritical point, T_{BCP}, are reached.

The dotted line in figure 4 gives the phase diagram with a field applied perpendicular to the c-axis. As anisotropy is being reinforced by the applied field H_{xy}, there is no spin-flop line, and therefore little detail to observe. It can be noted that for neither orientation could the SQUID apply a field close enough to the saturation field to cause the SF/paramagnetic (SF/P) line to bend back towards the H-axis. An estimate for the saturation field, H_{zs}, can be obtained from the anisotropy and exchange [13], and is found to be $\sim 1.8 \times 10^6$ Oe—far beyond any possible SQUID measurement. Similar calculations give the exchange field, H_e, as 0.9×10^6 Oe and the anisotropy field, H_a, as 1 kOe, giving $\alpha = H_a/H_e \approx 1 \times 10^{-3}$, agreeing with the statement that $MnPS_3$ is very close to being a Heisenberg system.

4. $Mn_xZn_{1-x}PS_3$

Measurements similar to those described above were repeated for $x = 0.95$, 0.8, 0.65, 0.5 and 0.3. Figure 5 shows $\chi_\parallel$ against T for the dilutions that showed a phase transition. The figure shows that the hump in the susceptibility at $T > T_N$ vanishes progressively with

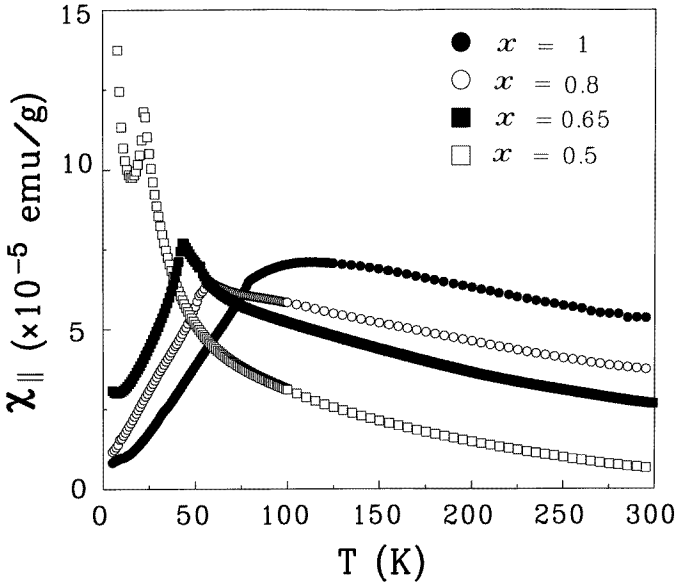

Figure 5. χ plotted against T for different values of x.

decreasing x, demonstrating the breakdown of correlations within the planes. At $x = 0.5$ there is a strong paramagnetic behaviour for small T, as now many of the spins no longer belong to the infinite cluster. The types of order appear to remain the same as in the pure material, although neutron scattering is needed to prove or disprove this.

The phase diagram for $x = 0.5$ is shown in figure 6. For $x = 0.3$, no ordering occurred.

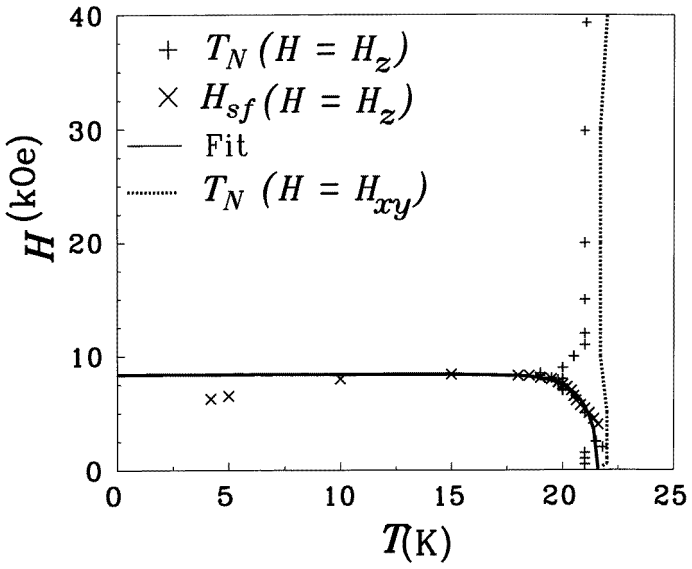

Figure 6. The magnetic phase diagram of $Mn_{0.5}Zn_{0.5}PS_3$.

Again, the dotted line gives the H_{xy} phase diagram. Because at $x = 0.5$ the anisotropy is greatly reduced, H_{xy} enhances the ordering interaction, and serves to increase T_N at a rate of 3.6×10^{-5} K Oe^{-1} for $H_{xy} > 25$ kOe.

An increase in the size of the critical region can be seen. While the material is now dilute and random, critical-region broadening requires macroscopic inhomogeneities. The results from [8] suggest that truly random examples of $Mn_xZn_{1-x}PS_3$ can be produced. And for the samples used here, XRD and microprobe experiments demonstrate that no such inhomogeneities exist in the material. Therefore, either the transition is sensitive to local inhomogeneity—unlikely given that correlation lengths diverge at a phase transition—or some other effect is at work. Reduced effective dimensionality could also broaden the phase transition, but there is little evidence to support this hypothesis. The question remains unresolved.

Random-field effects [4] could also affect the width of the critical region. However, the expected history dependence in the susceptibility has not been observed. If the dependence is weak, this could be masked by the high paramagnetic background. This background is the result of a large number of isolated magnetic atoms and clusters existing at small x. This limitation could be overcome using neutron scattering, as it probes the magnetic Bragg peaks directly. Alternatively, if second- and third-nearest-neighbour (nnn and 3nn respectively) interactions are significant, they could act to smooth the random-field effects. These effects would then become negligible until very high dilutions are reached, at which the magnetic order itself will have broken down. Figure 6 demonstrates that it is the SF line that bifurcates at the BCP. This is not always the case [19], and demonstrates that $Mn_{0.5}Zn_{0.5}PS_3$ is a good approximation to a 2D system. Whether the bifurcation behaviour depends on Zn content cannot be established with the resolution of the SQUID. Neutron scattering experiments in high fields may be necessary.

H_{sf} at low T still has the positive temperature dependence observed earlier, but the maximum is reached at a relatively lower temperature. This is because the dilution reduces the correlation length, resulting in the earlier onset of critical fluctuations. This also helps to explain the breadth of the critical region.

Of great interest is the very presence of order for $Mn_{0.5}Zn_{0.5}PS_3$. The critical concentration for site dilution in a honeycomb lattice with nearest-neighbour interactions is $p_c(s) = 0.7$ [20]. Thus if $Mn_xZn_{1-x}PS_3$ were describable by a nearest-neighbour exchange only, it should not order for $x = 0.5$. Reference [20] shows that for 3nn interactions, where $J_1 = J_2 = J_3$, $p_c(s) = 0.3$. Our results show order at $p = x = 0.5$ and none at $x = 0.3$. This suggests that J_2 and J_3 are significant but, as expected, weaker than J_1. This also agrees with the small reduction in T_N at H_{sf} in the pure material—nnn and 3nn interactions may well act to maintain the ordering.

Our figure of $T_N = 54$ K for $x = 0.8$ agrees very well with [8], which reports the same value from using a Faraday balance. That the continuance of order for $x < 0.7$ has not been noted in [8] is understandable, as the lowest temperature explored is 30 K. Also, a large paramagnetic signal appears at high dilution.

5. The 3D phase diagram

These results can be collected into a temperature/applied-field (H_z)/dilution magnetic phase diagram for $Mn_xZn_{1-x}PS_3$ (figure 7). Here, the enclosed region is the antiferromagnetic region. Above the top surface is the spin-flop phase, and climbing to large enough H_z would bring about a high-order phase transition to a paramagnetic aligned state. Coming out of the page, the system enters into a disordered paramagnetic state due to increasing

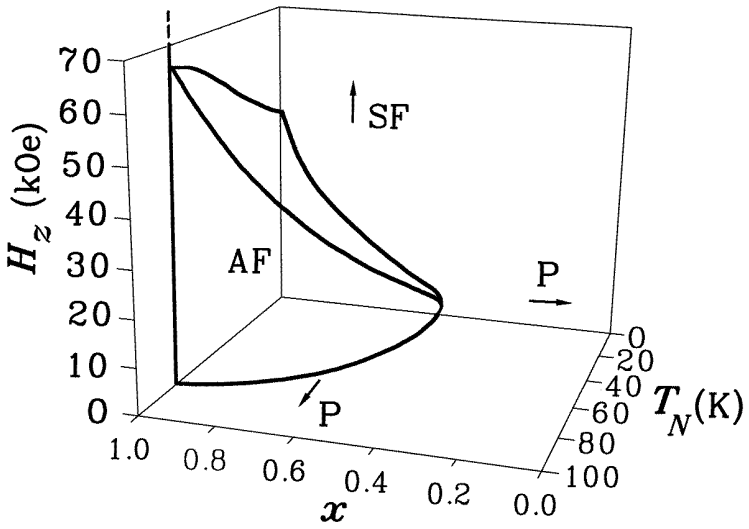

Figure 7. The temperature/applied-field ($H = H_z$)/dilution phase diagram for $Mn_xZn_{1-x}PS_3$.

temperature, while to the right it enters paramagnetism due to lack of magnetic atoms.

The shape of the T_N versus x curve for low field is projected onto the T_N–x plane. T_N obeys a linear decrease with x until approximately $x = 0.7$ (the nn percolation threshold) is reached and then proceeds to accelerate towards zero, reaching it for between 50 and 70% Zn.

According to [13] the SF and AF/P boundaries in figures 4 and 6 can be fitted to

$$\frac{T_N(H_z)}{T_N(0)} = \left(1 - \frac{H_z^2}{H_{sf}^2}\right)^n \tag{3}$$

where the term on the right-hand side is a measure of the effective anisotropy. These fits were performed, varying only n, and using the maximum value of H_{sf}. The fits for $x = 1$ and $x = 0.5$ can be seen as the full lines in figures 4 and 6 respectively. For $x = 1$, 0.8 and 0.5, n was found to be 0, 0.03 and 0.05 respectively, and so gives a measure of the broadening of the critical region away from a logarithmic dependence ($n = 0$) of T_N on the effective anisotropy. Allowing for the temperature dependence of H_{sf}, the fits are acceptable, again demonstrating the 2D nature of $Mn_xZn_{1-x}PS_3$.

6. Conclusions

We have constructed the $T/H_z/x$ phase diagram for $Mn_xZn_{1-x}PS_3$. From this work, we conclude that $MnPS_3$ is a good approximation to a 2D Heisenberg antiferromagnet with small Ising-like anisotropy.

The soliton theory put forward in [1, 13] appears useful in describing the spin-flop transition, although it breaks down in the critical region, probably due to a field dependence in q^{-1}. Furthermore, the spin-flop phase is a true LRO state, although this is to be explored further.

Also, care must be taken when analysing results, as a nearest-neighbour model does not appear to be sufficient. Interactions up to 3nn at least appear to be important in dealing with the magnetic properties.

Acknowledgments

Thanks to the Australian Research Council and the Australian Institute for Nuclear Science and Engineering for financial support. Thanks to Roman Liebach, former materials preparation officer in the Physics Department at Monash, for help in manufacturing the samples, and thanks to Dr Shane Kennedy of ANSTO and Dr Andrew Wildes of ILL for enlightening discussions.

References

[1] de Jongh L J (ed) 1990 *Magnetic Properties of Layered Transition Metal Compounds* (Dordrecht: Kluwer)
[2] Onsager L 1942 *Phys. Rev.* **65** 117–49
[3] Birgeneau R J, Guggenheim H J and Shirane G 1970 *Phys. Rev.* B **1** 2211–30
[4] Cowley R A, Aharony A, Birgeneau R J, Pelcovits R A, Shirane G and Thurston T R 1993 *Z. Phys.* B **93** 5–19
[5] Manousakis E 1991 *Rev. Mod. Phys.* **63** 1–62
[6] Kurosawa K, Saito S and Tamaguchi Y 1983 *J. Phys. Soc. Japan* **52** 3919–26
[7] Ouvrard G, Brec R and Rouxel J 1985 *Mater. Res. Bull.* **20** 1181–9
[8] Chandrasekharan N and Vasudevan S 1996 *Phys. Rev.* B **54** 14 903–6
[9] Okuda K, Kurosawa K, Saito S, Honda M, Yu Z and Date M 1986 *J. Phys. Soc. Japan* **55** 4456–63
[10] Wildes A R, Roessli B, Lebech B and Godfrey K W 1998 *J. Phys.: Condens. Matter* **10** 6417–28
[11] Rushbrooke G S and Wood P J 1958 *J. Mol. Phys.* **1** 257–83
[12] de Jongh L J 1972 *Proc. 18th Annu. Conf. on Magnetism and Magnetic Materials (Denver); AIP Conf. Proc.* **10** 561–5
[13] de Groot H J M and de Jongh L J 1986 *Physica* B **141** 1–36
[14] Landau D P and Binder K 1981 *Phys. Rev.* B **24** 1391–403
[15] Wildes A R, Kennedy S J and Hicks T J 1994 *J. Phys.: Condens. Matter* **6** L335–41
[16] Kosterlitz J M and Thouless D J 1973 *J. Phys. C: Solid State Phys.* **6** 1181–203
[17] Pich C and Schwabl F 1995 *J. Magn. Magn. Mater.* **148** 30–1
[18] Goossens D J and Hicks T J 1998 *J. Magn. Magn. Mater.* **177–181** 721–2
[19] Rauh H, Kullmann K, Gleik R, Erkelens W A C, Regnault L P and Rossat-Mignod J 1986 *J. Magn. Magn. Mater.* **54–57** 717–8
[20] Shante V K S and Kirkpatrick S 1971 *Adv. Phys.* **20** 325–57